

This is an Accepted Manuscript version of the following article, accepted for publication in:

J. Urrutia, M. Izquierdo, I. Ulacia, N. Agirre, I. Inziarte and J. Larrañaga, "Performance of the Counterbalance Systems in Heavy Industrial Robots Under Cyclic Operation," *2024 7th Iberian Robotics Conference (ROBOT)*, Madrid, Spain, 2024, pp. 1-6.

DOI: <https://doi.org/10.1109/ROBOT61475.2024.10797396>

© 2024 IEEE. Personal use of this material is permitted. Permission from IEEE must be obtained for all other uses, in any current or future media, including reprinting/republishing this material for advertising or promotional purposes, creating new collective works, for resale or redistribution to servers or lists, or reuse of any copyrighted component of this work in other works.

# Performance of the counterbalance systems in heavy industrial robots under cyclic operation

Julen Urrutia

*I+D Department*  
*Aldakin Automation S.L.*  
Alsasua, Spain  
jurrutia@aldakin.com

Mikel Izquierdo

*Mechanical and Industrial Production Dept.*  
*Mondragon Unibertsitatea*  
Mondragón, Spain  
mizquierdo@mondragon.edu

Ibai Ulacia

*Mechanical and Industrial Production Dept.*  
*Mondragon Unibertsitatea*  
Mondragón, Spain  
iulacia@mondragon.edu

Nora Agirre

*I+D Department*  
*Aldakin Automation S.L.*  
Alsasua, Spain  
n.agirre@aldathink.com

Ibai Inziarte

*I+D Department*  
*Aldakin Automation S.L.*  
Alsasua, Spain  
inziarte@aldathink.com

Jon Larrañaga

*Mechanical and Industrial Production Dept.*  
*Mondragon Unibertsitatea*  
Mondragón, Spain  
jlarranaga@mondragon.edu

**Abstract**—Industrial robot accuracy is limited in applications such as machining processes, mainly due to the relatively low stiffness of the joints. Deviations are caused by the weight of the links, external forces, inertias and the effects of the counterbalance system (CBS). The latter are hydropneumatic cylinders used to decrease motor torque and support the heaviest links. The counterbalance system influences joint torque and subsequently affects calculated deviations, making its behavior essential in robot positioning error models.

While position-dependent static isothermal counterbalance models are presented in the literature, the effects of repetitive use and subsequent temperature increases on the counterbalance systems have not been thoroughly analyzed. This study examines a counterbalance system, focusing on its behavior under cyclic performance and the subsequent temperature increase. Measurements indicate that the temperature increases with the cycles, causing a rise in pressure. The temperature rise does not remain constant with cycles, instead, it gradually decreases until it stabilizes. Additionally, it is observed that increasing the rotational speed of joint 2 also increases the temperature gain of the counterbalance system. This variation is seen to affect the final position of the robot's tip through the modification of the gearbox torque of the joint 2.

**Index Terms**—counterbalance, gravity compensator, industrial robot, cyclic effect, temperature

## I. INTRODUCTION

Industrial robots are playing an increasingly significant role in the manufacturing industry due to their versatility, extensive capabilities, and lower investment costs compared to traditional machine tools [1]–[3]. These benefits have enabled their deployment in high-value, complex tasks such as machining. Initially, the use of industrial robots was confined to non-processing activities like handling, assembly, and welding, which do not typically require high precision. However, performing precision-intensive operations remains a considerable challenge for existing robotic technologies [4]–[8].

Heavy industrial robots, commonly used in machining operations, often are equipped with a counterbalance system to mitigate gravitational forces. Traditionally, these systems have

relied on mechanical springs [9]. However, currently, most of the counterbalance mechanisms are based on hydropneumatic cylinders, in order to more effectively counteract gravity's impact on robotic arms [10]. These systems typically consist of a hydropneumatic cylinder connected to the largest joint that holds most of the own weight. The rotational movement of this joint causes a linear motion in the cylinder piston, altering the chamber pressure and consequently varying the force and torque applied to the joint [11]. This integration offsets the gravitational effects on the joint, with the counterbalance system aligning with the joint when the link is vertical, thereby preventing additional torque. As the joint moves away from that point, the counterbalancing effect becomes more pronounced. The correct functioning of the counterbalance system is essential for maintaining the accuracy and repeatability of the robot's movements, influencing the torque of the affected joint. Despite its significance, the counterbalance system remains understudied, with limited research examining its impact on the performance of industrial robots.

Klimchik et al. [12] introduced a first model describing the counterbalance system, highlighting how the angular position of the joint directly influences the cylinder volume, pressure and ultimately the force and torque applied to the joint. In this counterbalance system model, a constant temperature (isothermal) and an ideal gas was considered to estimate the gas pressure.

Same counterbalance system model has been employed in other works to identify the robot position dependant stiffness based on the estimation of joint torque [13], [14]. Besides, Xu et al. [14] used this counterbalance system model to highlight the importance of the counterbalance system in the robot's positional accuracy and they exposed that the counterbalance system has a significant influence in the robot's tip deflection. However, none of the works have deepened into the functioning of the counterbalance system, assuming the initial hypotheses proposed by the model.

On the other hand, in hydropneumatic cylinders, energy losses can occur due to fluid friction, viscosity, and other inefficiencies within the system, especially notable with the increase of the velocity. These losses manifest as heat, contributing to an increase in temperature of the hydraulic fluid. Finally, this residual heat is transmitted to the gas, causing it to expand and leading to an increase in its pressure [15], [16].

For instance, Els et al. [17] subjected a hydropneumatic suspension to a excitation trajectory with a frequency of 0.5 Hz and amplitude of 60 mm and observed a temperature variation of up to 50°C, showing that assuming a constant temperature can lead to large errors in pressure prediction. Although the temperature of hydropneumatic cylinders can increase during repetitive applications, none of the studied counterbalance models have considered this effect, nor have they analyzed its impact on the robot's positional accuracy.

As a result, the objective of this work is to analyze the effect of temperature increase in the counterbalance system on the robot's performance. To do this, temperature, pressure and torque of the gearbox are measured by subjecting the robot to a cyclic and constant movement, and then analyzing the influence of that temperature on the robot's operation.

To achieve these objectives, this paper is structured into five other sections. In Section II the operation of the counterbalance system is described, along with the geometry by which it is governed. Then, in Section III, the studied robot and the setup used for the experimental tests are presented, while in Section IV, the tests conducted to analyze the cyclic effect on the counterbalance system are described. Finally, the results obtained from these tests and the derived discussion are presented in Section V and the conclusions drawn from the study are presented in Section VI.

## II. MODEL OF THE COUNTERBALANCE SYSTEM

The counterbalance system is a mechanism that acts on the joint most requested by the own weight of the robot, to which it is coupled to apply a torque that counteracts that load. It is a hydropneumatic cylinder whose piston moves at the same time with the rotation of the joint. Fig. 1 shows the configuration of this system in the robot, as well as the characteristic points and the parameters that define the geometry that relates the movement of the piston to the joint.

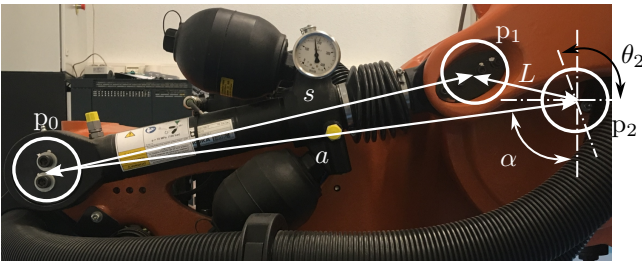


Fig. 1: Geometry of the counterbalance system

The point  $p_0$  is the junction of the system with the base, whose relative motion with respect to the joint is zero. The

point  $p_1$  is where the mechanism attaches to one end of the joint, which will rotate along with the joint. Finally,  $p_2$  is the center of revolution of the joint. As the joint rotates, the point  $p_1$  rotates with it, pulling or compressing the mechanism, thus regulating the force and moment applied to the joint.

As far as the geometry is concerned,  $a$  corresponds to the distance between joint 2 ( $p_2$ ) and the fixed point ( $p_0$ ) of the counterbalance system ( $\overline{p_0p_2}$ ),  $L$  is the distance between joint 2 ( $p_2$ ) and the moving point ( $p_1$ ) of the counterbalance system ( $\overline{p_1p_2}$ ),  $\alpha$  is the misalignment angle between joint 2 ( $p_2$ ) and the fixed point ( $P_0$ ) of the counterbalance system ( $\tan \frac{a_y}{a_x}$ ), and  $s$  is the distance between the fixed point and the moving point ( $p_1$ ) of the counterbalance system ( $\overline{p_0p_1}$ ) representing linear position/elongation variable. Using trigonometric operations, the relationship between the angular joint position ( $\theta_2$ ) and the linear position of the piston ( $s$ ) is deduced, according to the equation. (1).

$$s^2 = a^2 + L^2 + 2aL \cos(\alpha - \theta_2) \quad (1)$$

To calculate the torque exerted by the counterbalance system, it is necessary to consider the gas pressure inside the cylinder. For a closed cylinder with a constant amount of matter, the ideal gas (Eq. (2)) can be utilized. The models developed so far consider a constant temperature (isothermal process), eliminating that factor [12]–[14]. However, when the system is subjected to continuous operation, it is possible that the temperature can vary, altering the pressure.

$$\frac{PV}{T} = \frac{P_0V_0}{T_0} \quad (2)$$

Here,  $P$  represents gas pressure,  $V$  gas volume and  $T$  gas temperature, while subscript 0 denotes initial conditions. The gas pressure depends inversely on the gas volume, which changes proportionally to the area of the cylinder (Eq. (3)), and directly on the temperature of the gas.

$$V = \frac{\pi}{4}(d_{\text{piston}}^2 - d_{\text{rod}}^2)(s_0 - s) + V_0 \quad (3)$$

From these equations, Klimchik et al. [12] presented the first model that predicted the gas pressure (quasistatic pressure) considering an isothermal process (constant temperature). However, when the system is subjected to continuous operation, it is possible that the temperature varies, altering the pressure. Therefore, this effect has been added to the existing model, according to Eq. (4).

$$P(\theta_2, T) = \frac{4P_0V_0}{\pi(d_{\text{piston}}^2 - d_{\text{rod}}^2)\sqrt{s_0^2 - s^2 + 4V_0}} \cdot \frac{T}{T_0} \quad (4)$$

Where,  $d_{\text{piston}}$  is the diameter of the piston,  $d_{\text{rod}}$  is the diameter of the rod and  $\theta_2$  is the angular position of the joint.

By knowing the internal pressure of the cylinder, the force applied by the piston can be obtained, and by means of the proposed geometric relationships, the torque exerted on the joint is obtained, according to the Eq. (5).

$$M_{CBS} = P(\theta_2, T) \frac{\pi}{4} (d_{\text{piston}}^2 - d_{\text{rod}}^2) \frac{La}{s(\theta_2)} \sin(\alpha - \theta_2) \quad (5)$$

Finally, the total torque perceived by the joint 2 ( $M_2$ ) is considered as the sum of the gearbox torque ( $M_{2\text{GBX}}$ ) and the torque applied by the counterbalance system ( $M_{CBS}$ ), as shown in Eq. (6).

$$M_2 = M_{2\text{GBX}} + M_{CBS} \quad (6)$$

### III. INDUSTRIAL ROBOT

The robotic arm employed in this study is a 6 link Kuka KR270 R2700 Quantec Ultra (Fig. 2). The analyzed hydropneumatic counterbalance is GA12-A 00179516 00-179-51 model, provided with the robot by the manufacturer KUKA. The counterbalance cylinder is attached between links 1 and 2, aiding joint 2 of the robot in counterbalancing the weight or masses that need to be lifted. According to the documentation of the robot the counterbalance system applies a null torque when the joint 2 is positioned at  $-90^\circ$ , as this is the point at which the adjacent link aligns vertically.

To analyze the behavior of the counterbalance system the pressure inside the cylinder was observed. For this purpose, a pressure gauge SCP01-400-24-07 from Parker, with a maximum error of  $\pm 0.5$  bar was installed in one of the cylinder pressure control valves. A type K thermocouple has also been installed in the middle of the stroke of the piston of the cylinder to observe the temperature evolution throughout the cycles. All of this is shown in Fig. 2. In addition, it should be noted that the robot is in a controlled environment where the temperature is maintained at around  $23^\circ\text{C}$ .

The torque exerted on the gearbox of the joint 2 ( $M_{2\text{GBX}}$ ) was obtained from the internal data of the KRC4 controller, which measures torque based on the motor current and considering the reduction ratio of the transmission chain ( $i = 266.56$ ). The geometric and cylinder parameters (Section II) corresponding to the counterbalance system of the presented robot are gathered in Table I.

TABLE I: Geometric and cylinder parameters of the counterbalance system

Parameter	Value	Parameter	Value
$a$ [mm]	$806.79 \pm 0.015$	$d_{\text{piston}}$ [mm]	52.00
$L$ [mm]	$203.01 \pm 0.015$	$V_0$ [l]	1.19
$\alpha$ [ $^\circ$ ]	$85.08 \pm 0.8$	$P_0$ [bar]	169.642
$d_{\text{rod}}$ [mm]	30.00	$T_0$ [ $^\circ\text{C}$ ]	$23 \pm 1$

### IV. CYCLIC OPERATION TESTS

In order to observe the evolution of the temperature, internal pressure of the counterbalance system over time with cyclic use of the robot, the following tests were carried out. The robot was positioned in the poses of Fig. 3 and the joint 2 was rotated between  $-130^\circ$  and  $-10^\circ$  in both directions. Table II shows the positions of the joints.

To observe how the effect of cycles changes based on the speed at which the joint moves, these movements have been

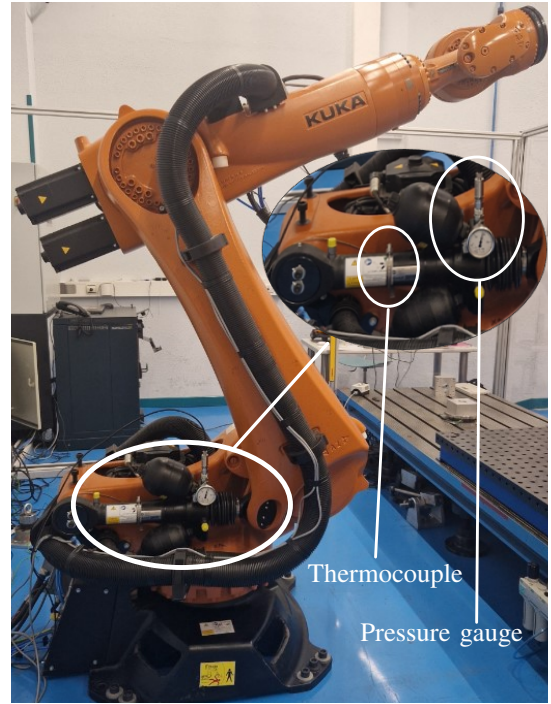


Fig. 2: Kuka KR270 R2700 Quantec Ultra, SCP01-250-24-07 pressure gauge and K thermocouple

TABLE II: Position of the joints in the tests

Joint	Position [ $^\circ$ ]	Joint	Position [ $^\circ$ ]
1	54	4	0
2	$-130/-10$	5	0
3	0	6	0

performed at 3, 10, 30 and 50 %s, with 200 repetitions of each. Every 20 repetitions, a cycle at 0.5 %s was performed to measure the quasistatic pressure of the cylinder, minimizing the dynamic effects of the robot on the pressure. Three repetitions of the heating-up movement were performed, and the pressure and temperature values were averaged on the results.

### V. RESULTS AND DISCUSSION

Fig. 4 illustrates the evolution of the temperature of the hydropneumatic cylinder as the number of cycles increases at 4 different speeds, relative to its initial temperature of  $23^\circ\text{C}$  ( $T/T_0$ ).

The temperature rises while increasing the number of cycles in all the speeds. However, the rate of the temperature increase diminishes over time, as the curve begins to stabilize. Additionally, it is evident that speed significantly influences the temperature evolution. Specifically, the temperature increase per cycle is higher at greater speeds. Consequently, higher speeds result in higher final temperatures, as the stabilization temperature also rises. At the lowest speed, the temperature increases by up to 1.3%, reaching  $28^\circ\text{C}$ , while at the highest speed, the increase is 4%, reaching  $40^\circ\text{C}$  in the cycle 200. Fig. 5 shows the pressure curve for the first cycle and the pressure

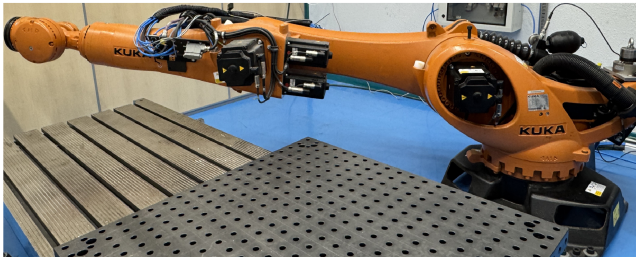
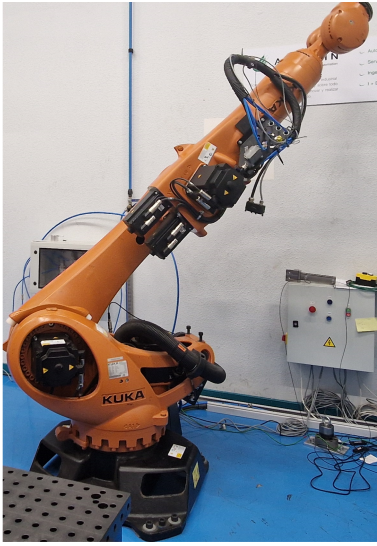


Fig. 3: Initial and final position of the robot during the tests

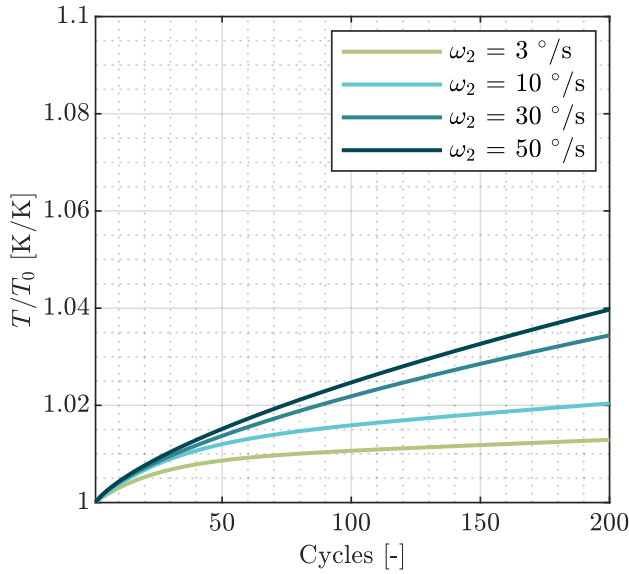


Fig. 4: Evolution of temperature as a function of the number of cycles

differences for each subsequent measurement compared to the first cycle from tests conducted at 3 %/s.

It can be observed that as the number of cycles increases due to the temperature rise, the pressure difference ( $\Delta P$ ) also increases for the entire trajectory. This is in agreement

with the assumption of considering the internal gas of the counterbalance system as ideal. Additionally, the results show that the difference between the pressure curves increases with the number of cycles, which is consistent with the stabilization seen in the evolution of the temperature. It should be noted that the pressure difference along the stroke is not constant, likely due to internal mechanisms of the hydropneumatic cylinder itself, which causes slight variations at certain points of the stroke of the piston.

The torque exerted by the counterbalance systems on joint 2 ( $M_{CBS}$ ) was calculated using Eq. (5) with the experimentally measured pressure at 3 %/s (Fig. 6). As expected, the torque increases in proportion to the rising pressure. It can be observed that as the joint position deviates from the alignment point ( $\theta_2 = -95.92^\circ$ ), where the force from the cylinder aligns with the joint's center of rotation and thus results in zero torque, the differences in torque become more pronounced. This is due to the geometry of the system, which amplifies the force exerted by the cylinder on the torque applied at the joint in the positions farthest from the neutral point.

To determine if this phenomenon affects the robot's performance, the evolution of the motor torque for joint 2 over multiple cycles was analyzed ( $M_{2GBX}$ ). Similar to the pressure analysis, Fig. 7 shows the torque during the first cycle and the difference in torque over subsequent cycles at a joint speed of 3 %/s. The variation of torque increases with the cycles, which confirms the effect of the temperature in the counterbalance system in the robot's performance. Additionally, the torque exerted by the counterbalance system rises until 120 Nm, while the torque of the gearbox reaches 111.4 Nm, what indicates a direct relationship. It is worth mentioning that the increase in torque exerted by the counterbalance system ( $M_{CBS}$ ) reduces the workload on the joint 2 (Eq. (2)), what reduces the torque applied by the motor ( $M_{2GBX}$ ), resulting in negative values.

Relating the increase in temperature to pressure and its effect on the motor of joint 2, it is observed that a rise in temperature increases the torque exerted by the counterbalance system and decreases the torque experienced by joint 2. For example, at a rotational speed of 3 %/s, the temperature increases by up to 1.7% (5°C) by cycle 200, leading to a pressure variation of nearly 3 bar (a 1.77% increase compared to  $P_0$ ) and a maximum increase of 120 Nm in the torque exerted by the counterbalance system (at a position of  $-10^\circ$  for joint 2).

The results show that the variation in the torque of the gearbox of joint 2 caused by the temperature fluctuation may be considered in correction models based on stiffness of the robot joints, as the calculated deviation is directly proportional to the torque applied [12]–[14]. Therefore, after verifying the effect of the temperature of the counterbalance system on the torque of joint 2, it is necessary to understand how this effect translates to the positional accuracy of the robot's tip. To achieve this, the maximum deviation caused by this variation has been calculated. This maximum deviation has been obtained at the position of the robot where it achieves its maximum reach (2969 mm) which corresponds with the

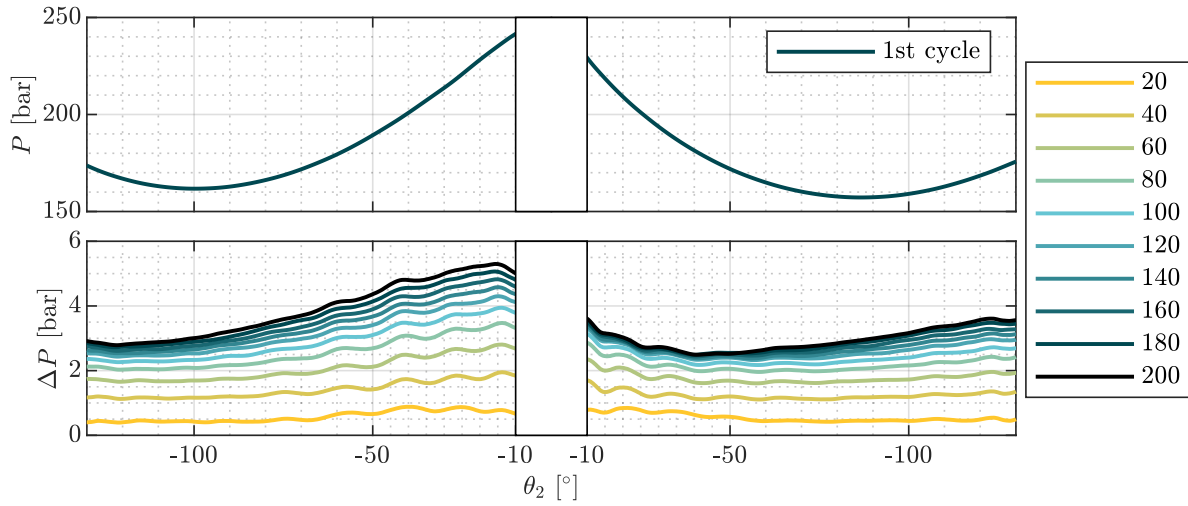


Fig. 5: Gas pressure in the first cycle and the difference by number of cycles at 3%/s

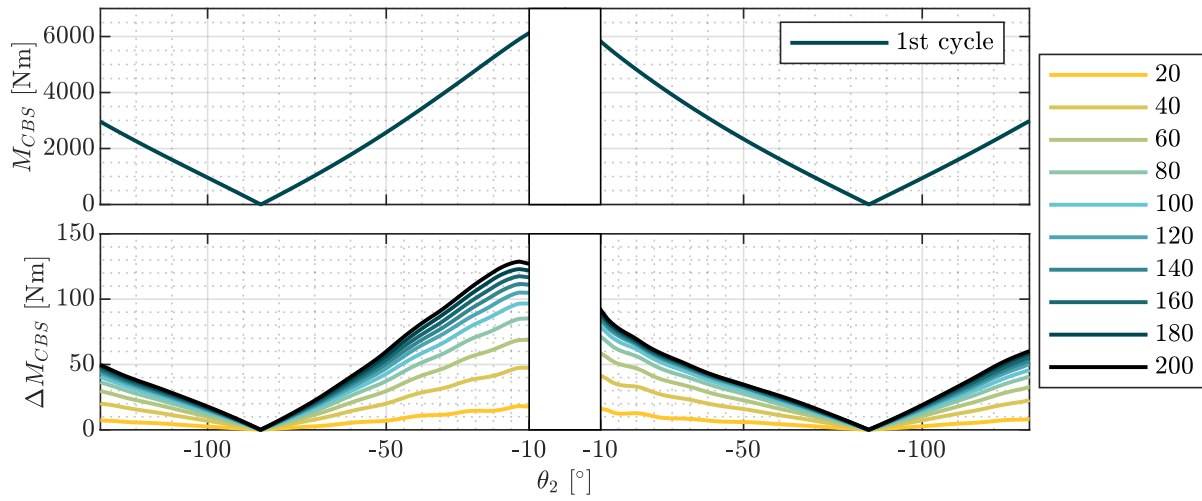


Fig. 6: Torque calculated of the joint 2 in the first cycle and the difference by number of cycles at 3%/s

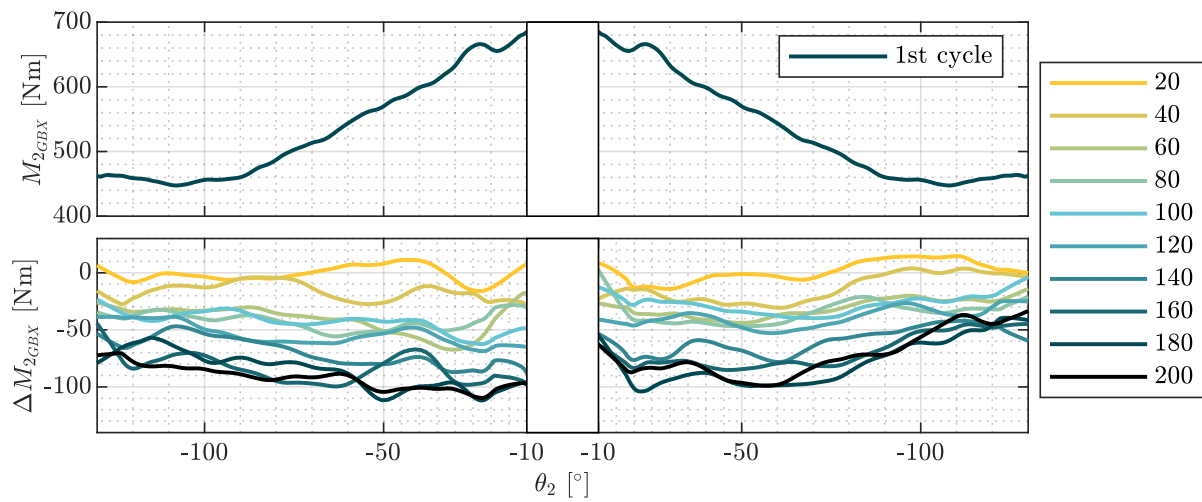


Fig. 7: Torque of the gearbox of the joint 2 in the first cycle and the difference by number of cycles at 3%/s

final position in Fig. 3 ( $\theta_2 = -10^\circ$ ), where the gearbox torque is 111.4 Nm at the 3 %/s speed. The stiffness used for the calculation is  $3.3113 \times 10^6$  Nm/rad, which has been obtained from a characterization done for the same robot model [9] and the deviation resulted in 0.01 mm. Besides, it has been observed that as the speed increases, the increase in temperature is greater. Therefore, considering that the increase at 50 %/s in cycle 200 is almost four times that at 3 %/s, the deviation would rise to 0.04 mm. It is also worth mentioning that at this maximum speed, temperature stabilization has not been reached yet, so with a higher number of cycles, the deviation would tend to increase.

Xu et al. [14] broke down the deviations of a robot into two different factors in the same position. They estimated that the robot's own weight caused a deviation of 8 mm. Meanwhile, based on Klimchik's counterbalance system model, they estimated that the counterbalance system caused a deviation of 6 mm.

Therefore, the deviation due to temperature variation in the counterbalance system is very small compared to both the influence of the robot's own weight and the isothermal effect of the counterbalance system. However, it can be significant in applications where high precision and high speed repetitive operations are required.

Additionally, if a robot is to be used for continuous work, it can be interesting carrying out a warming phase, taking into account the speed at which the task will be performed and considering the steady state temperature of the counterbalance system to correct the deviation of the tip. Besides, it also implies that robots operating at higher speeds may require additional cooling mechanisms or rest periods to prevent overheating and ensure consistent performance. Moreover, it would be recommendable to consider this effect both in the design and calibration process of the system and in its maintenance.

## VI. CONCLUSIONS

The impact of temperature increase in the counterbalance system on the robot's performance was evaluated. To assess this, temperature, pressure, and gearbox torque were measured while the robot was subjected to cyclic and constant movements. The influence of temperature on the robot's overall performance and these measurements were analyzed. Finally, the following conclusions were drawn:

- The counterbalance system has been subjected to continuous and cyclical movement. It has been observed that with the cycles, the temperature in the cylinder increases, which leads to an increase in pressure. This causes a variation in the force applied by the piston of the counterbalance system, what causes an increase in the exerted torque by the counterbalance system. This causes a reduction in the torque demanded from the motor, as proved by the experimental measurements.
- Furthermore, the evolution of this temperature shows a stabilization. However, as the speed increases, the temperature rises faster and reaches higher values before

stabilizing. In addition, the temperature curve shows that the velocity increases the cycles needed to reach the stabilization temperature.

- Finally, it has been observed that the effect of temperature on the counterbalance system, although it influences the positional accuracy of the robot, is very small compared the isothermally estimated pressure of the gas, as well as other factors such as the own weight of the robot.

## ACKNOWLEDGMENT

This research was partially supported by the Basque Government through the Bikaintek Program (ref. 020-B2/2020), the RobPosDig project of the UE program (ref. PUE\_2024\_1°\_0019), and the Aurrera project under the Elkartek program (ref. KK-2024/00024).

## REFERENCES

- [1] W. Ji, L. Wang, Industrial robotic machining: a review, *International Journal of Advanced Manufacturing Technology*, vol. 103(1–4), pp. 1239–1255, 2019.
- [2] Y. Chen and F. Dong, Robot machining: Recent development and future research issues, *International Journal of Advanced Manufacturing Technology* 66, 2013, pp. 1489–1497.
- [3] K. Wu, J. Li, H. Zhao, Y. Zhong, Review of Industrial Robot Stiffness Identification and Modelling, *Applied Sciences*, 2022.
- [4] T. Kubela, A. Pochyly, V. Singule, Assessment of industrial robots accuracy in relation to accuracy improvement in machining processes, *IEEE International Power Electronics and Motion Control Conference (PEMC)*, 2016, pp. 720–725.
- [5] M. Guillo, L. Dubourg, Impact improvement of tool deviation in friction stir welding: Weld quality real-time compensation on an industrial robot, *Robotics and Computer-Integrated Manufacturing* 39, 2016, pp. 22–31.
- [6] B. Denkena, T. Lepper, Enabling an Industrial Robot for Metal Cutting Operations, *Procedia CIRP* 35, 2015, pp. 79–84.
- [7] S. H. Kim, E. Nam, T. I. Ha, S. H. Hwang, J. H. Lee, S. H. Park and B. K. Min, Robotic Machining: A Review of Recent Progress, *International Journal of Precision Engineering and Manufacturing*, vol. 20, issue 9, pp. 1629–1642, 2019.
- [8] C. Doukas, I. Pandremenos, P. Stavropoulos, *Machining with Robots: A Critical Review*, 7th International Conference on Digital Enterprise Technology, Sept. 2011.
- [9] A. Klimchik, Y. Wu, C. Dumas, S. Caro, B. Furet, A. Pashkevich, and , Identification of geometrical and elastostatic parameters of heavy industrial robots, *IEEE International Conference on Robotics and Automation*, 2013.
- [10] V. Arakelian, Gravity compensation in robotics, *Advanced Robotics* 30, 2015, pp. 1–18.
- [11] G. Merk, A. Bayer, Industrial robot with a weight balancing system, patent US10987817B2, April 27, 2021.
- [12] A. Klimchik, A. Pashkevich, S. Caro and B. Furet, Calibration of industrial robots with pneumatic gravity compensators, *IEEE International Conference on Advanced Intelligent Mechatronics (AIM)*, Munich, Germany, 2017, pp. 285–290.
- [13] K. Yang, W. Yang, G. Cheng and B. Lu, A new methodology for joint stiffness identification of heavy duty industrial robots with the counterbalancing system, *Robotics and Computer-Integrated Manufacturing*, vol 53, 2018, pp. 58–71.
- [14] P. Xu, X. Yao, S. Liu, H. Wang, K. Liu, A. Senthil Kumar, W. Feng Lu and G. Bi, Stiffness modeling of an industrial robot with a gravity compensator considering link weights, *Mechanism and Machine Theory*, vol. 161, 2021.
- [15] W. Bauer, *Hydropneumatic Suspension Systems*, 4th edn, pp. 95–140. Springer, Heidelberg, 2011.
- [16] J. Dixon, *The Shock Absorber Handbook*, Premiere Series Books, Society of Automotive Engineers, 1999.
- [17] P. S. Els, B. Grobbelaar, Heat transfer effects on hydropneumatic suspension systems. *Journal of Terramechanics*, 1999.